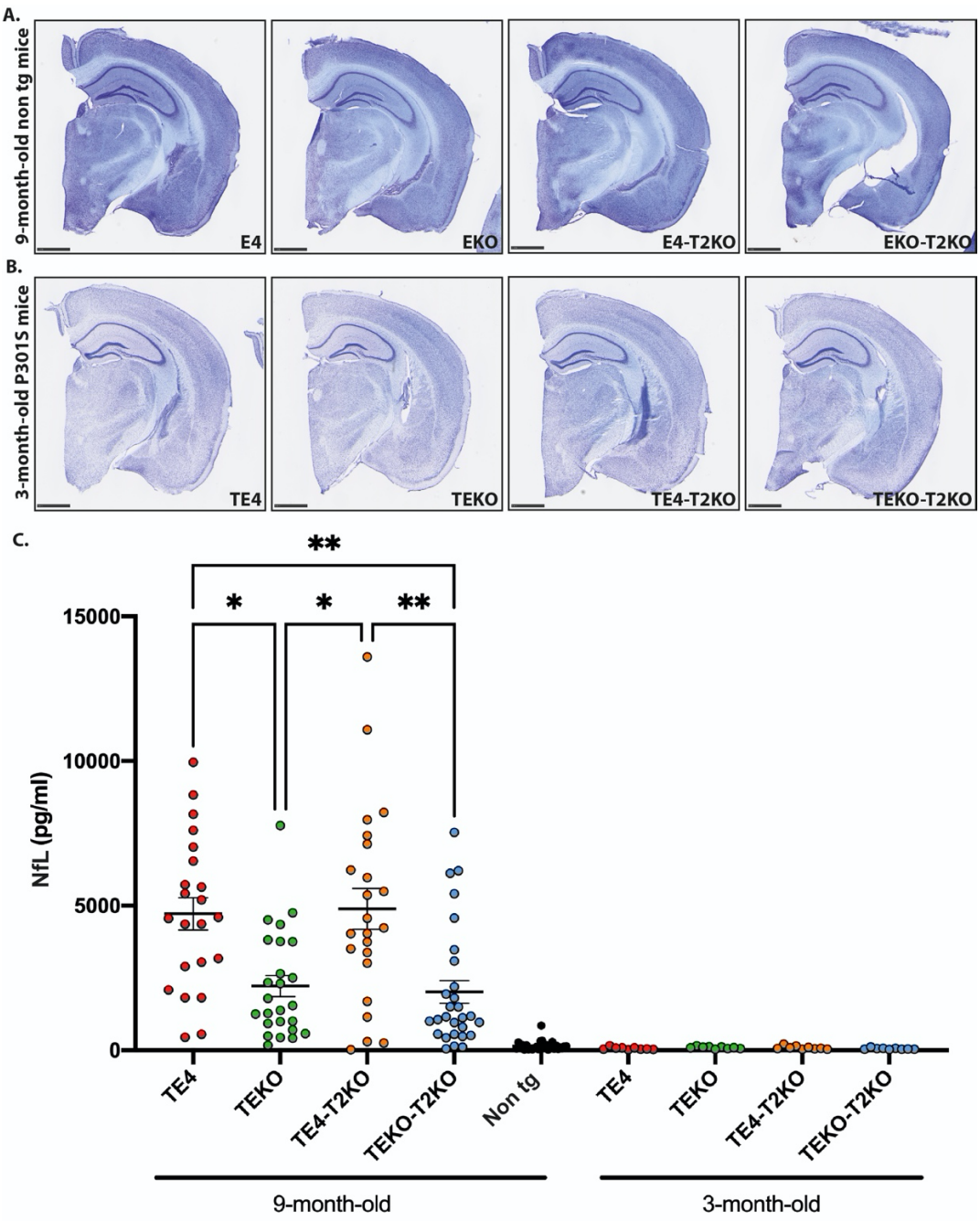

Suppl. Figure 1. Absence of neurodegeneration in 3-month-old TE4 and TEKO or in 9-month-old E4 and EKO mice with or without TREM2 (related to Figure 1).

(A, B) Representative images of Nissl staining from brains of non-P301S tau transgenic (non tg) 9-month-old E4 and EKO (A) and 3-month-old and TE4 and TEKO (B) mice with or without TREM2. Scale bars: 1 mm. (C) Quantification of neurofilament light chain levels (NfL) 9-month-old non-tg (including E4, E4-T2KO, EKO and EKO-T2KO mice; n=7-8/group), TE4 and TEKO and 3-month-old and TE4 and TEKO with or without TREM2. 9-month-old non tg and 3-month-old and TE4 and TEKO with or without TREM2 were not included in the statistical analysis. Data are presented as mean ± SEM. Significance was determined using a Kruskal–Wallis test followed by a Dunn's post hoc test due to the nonparametric data set. *, $P < 0.05$; **, $P < 0.01$. (n=9-27 mice/group).

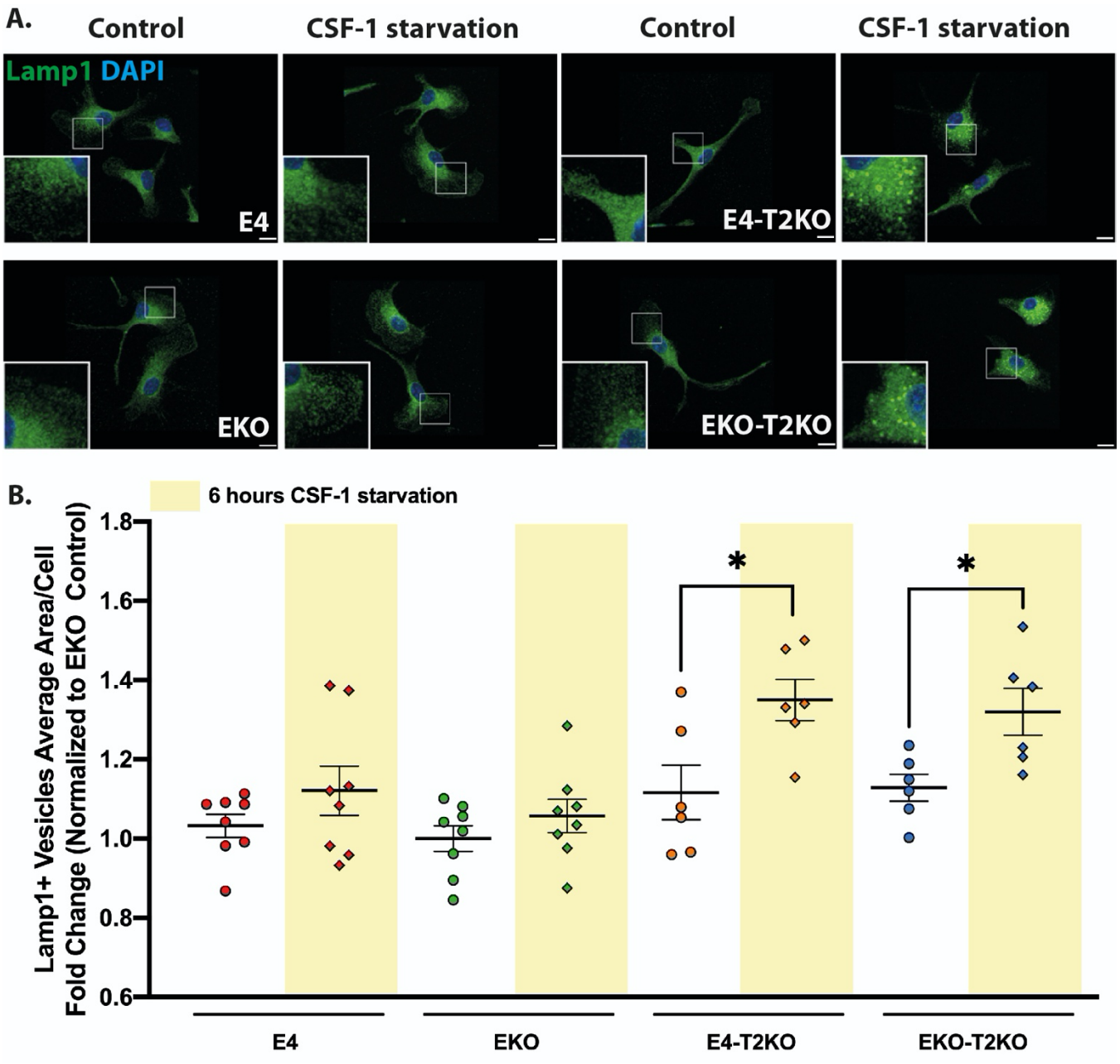

Suppl. Figure 2. Loss of TREM2 stimulates lysosomal volume after CSF-1 starvation *in vitro*, independently from ApoE (related to Figure 5). (A) Representative images of LAMP1 (green) and DAPI (blue) from Bone marrow-derived macrophages (BMDMs) starved or not for CSF-1 for 6 hours. Scale bars: 10 µm. (B) Fold change of Lamp1+ vesicles average area/cell normalized on EKO control (n=3-4 biological replicates in technical duplicates). Data are presented as mean ± SEM. Significance was determined using an unpaired, 2-tailed Student's t test for. *, $P < 0.05$; **, $P < 0.01$.

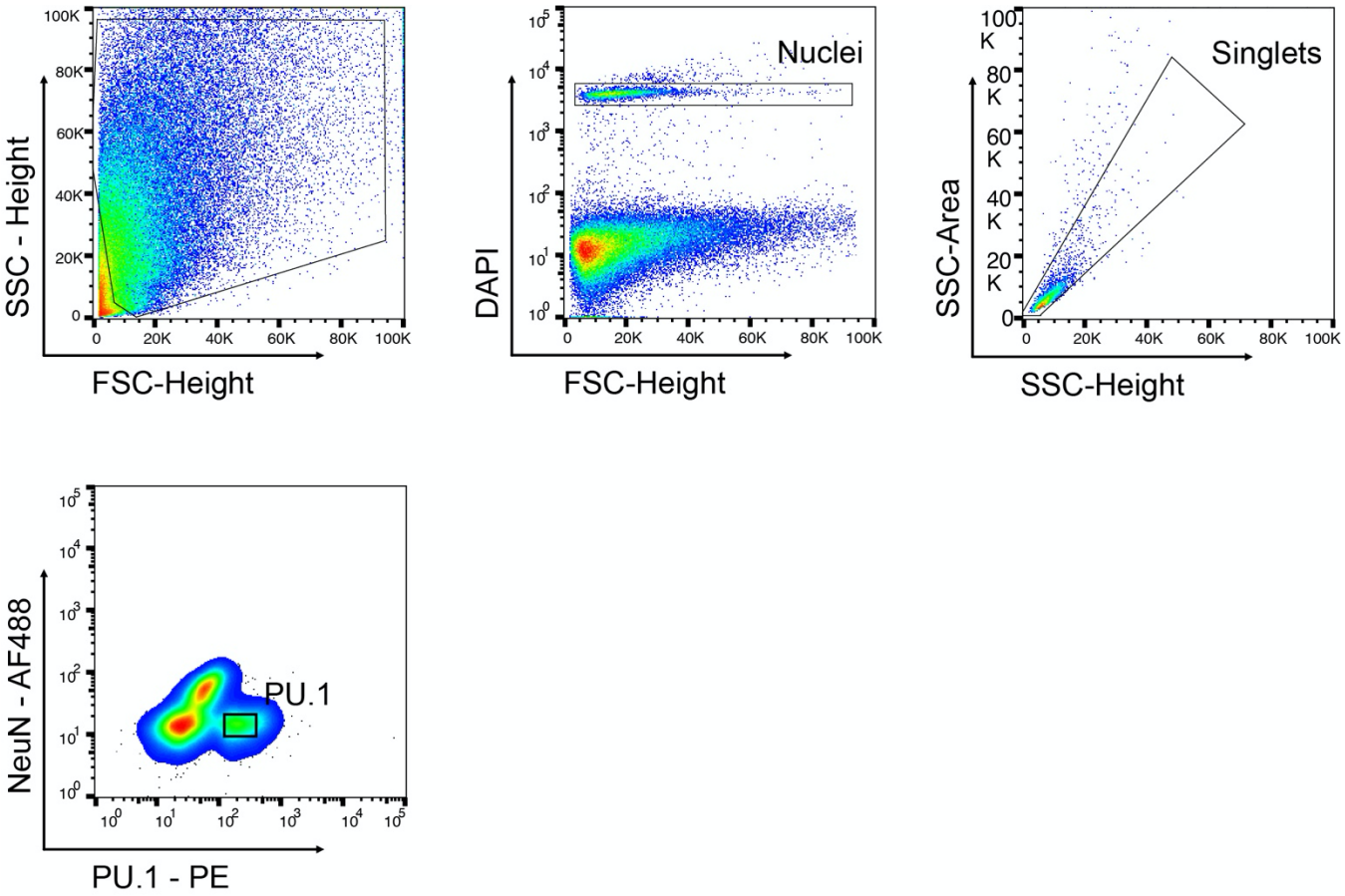

Suppl. Figure 3. FANS gating strategy for single nuclei RNA-sequencing (related to Figure 3). After dissociation and removal of myelin and debris from the mouse hippocampus, nuclei were stained for DAPI followed by staining for the neuronal and myeloid nuclei markers NeuN and PU.1, respectively. PU.1 positive myeloid nuclei were sorted and processed for downstream snRNA-seq or ATAC-seq.

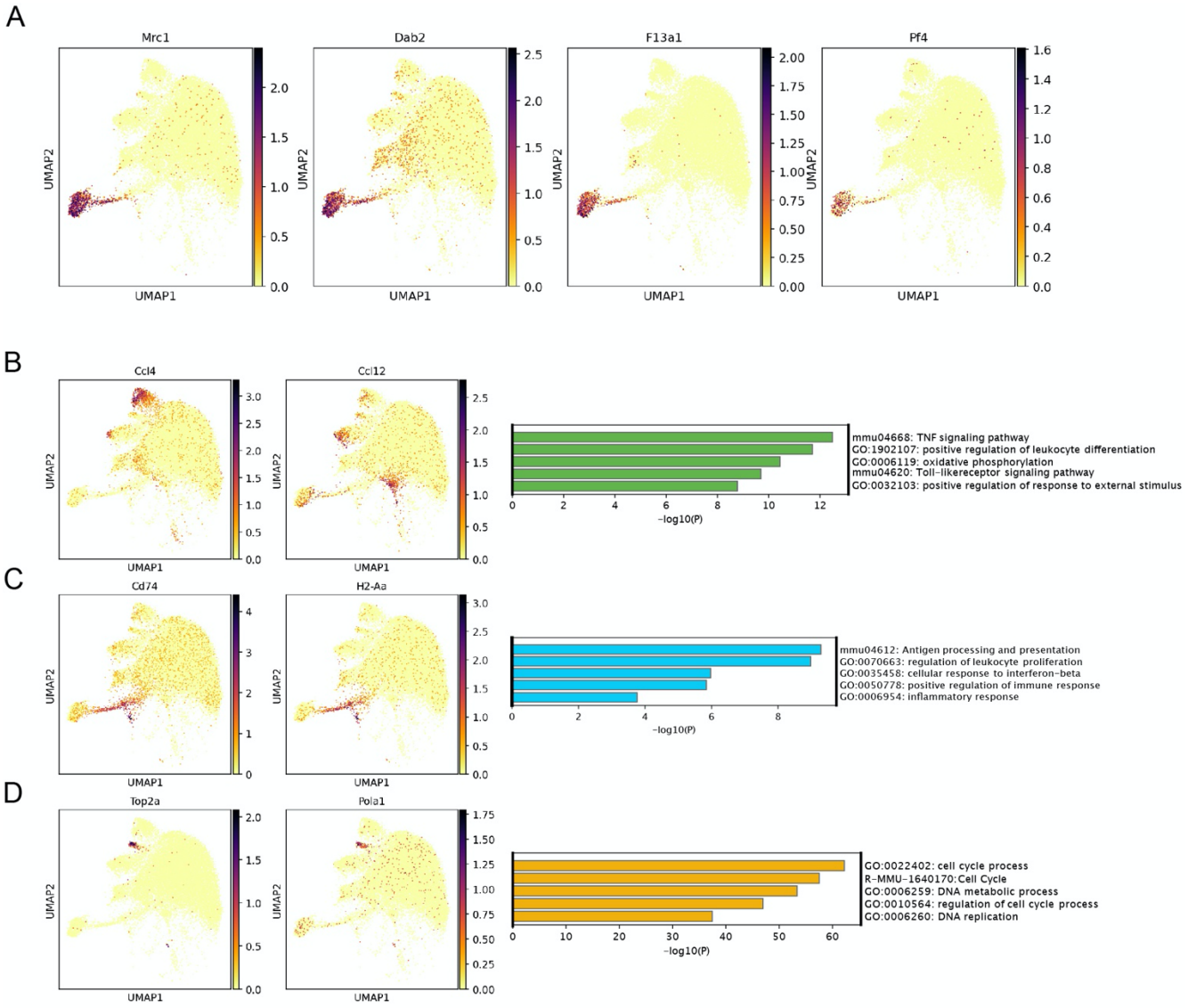

Suppl. Figure 4. Cluster specific marker gene expression for microglia clusters (related to Figure 3). (A) UMAP representation of macrophage markers Mrc1, Dab2, F13a1, and Pf4. (B) UMAP of selected genes (Ccl4, Ccl12) and GO analysis of significantly upregulated genes in inflammatory microglia. (C) UMAP of Cd74 and H2-Aa and GO analysis of MHCII microglia. (D) UMAP (Top2a, Pola1) and GO analysis of genes significantly upregulated in proliferating microglia.

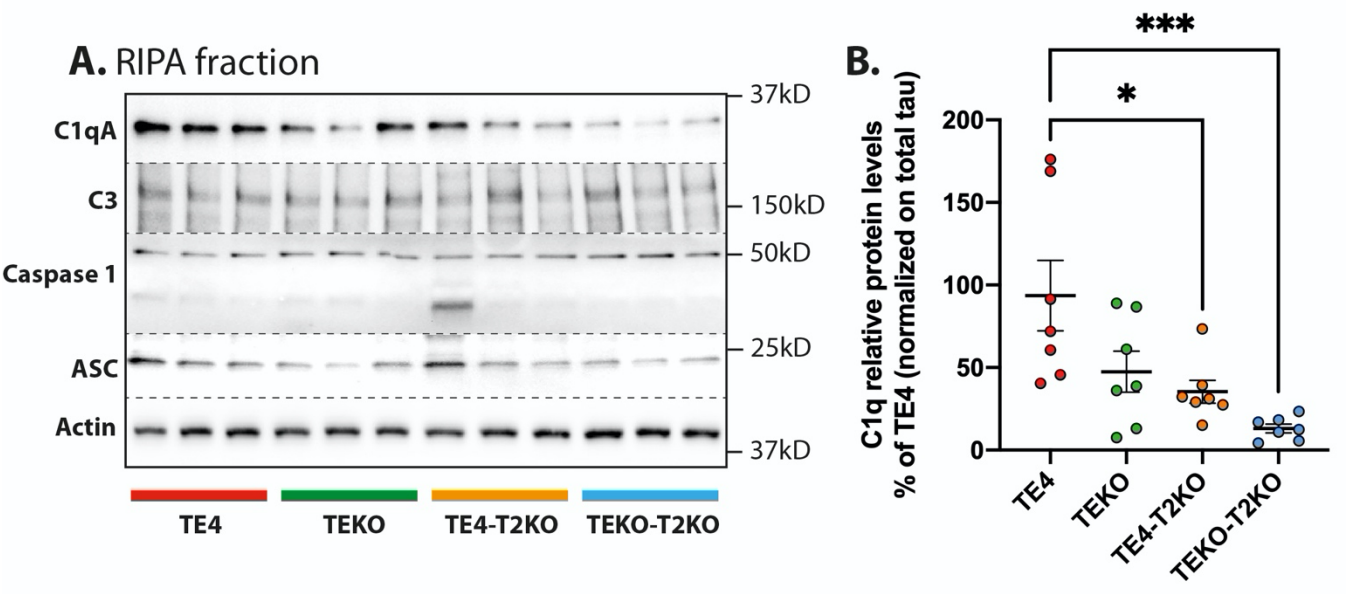

Suppl. Figure 5. Decrease of C1q in P301S Tau Tg mice in the absence of TREM2 (related to Figure 6). (A) Western blot detection of C1qA, C3, Caspase 1, ASC, and actin protein levels in RIPA fraction extracted from hippocampal tissue (3 representative lanes/group). (B) Quantitative analysis of C1qA relative levels in RIPA fraction (n=7 mice/group). Data are presented as the mean ± SEM. Significance was determined using a one-way ANOVA followed by a Tukey's post hoc test. *, $P < 0.05$; ***, $P < 0.001$.

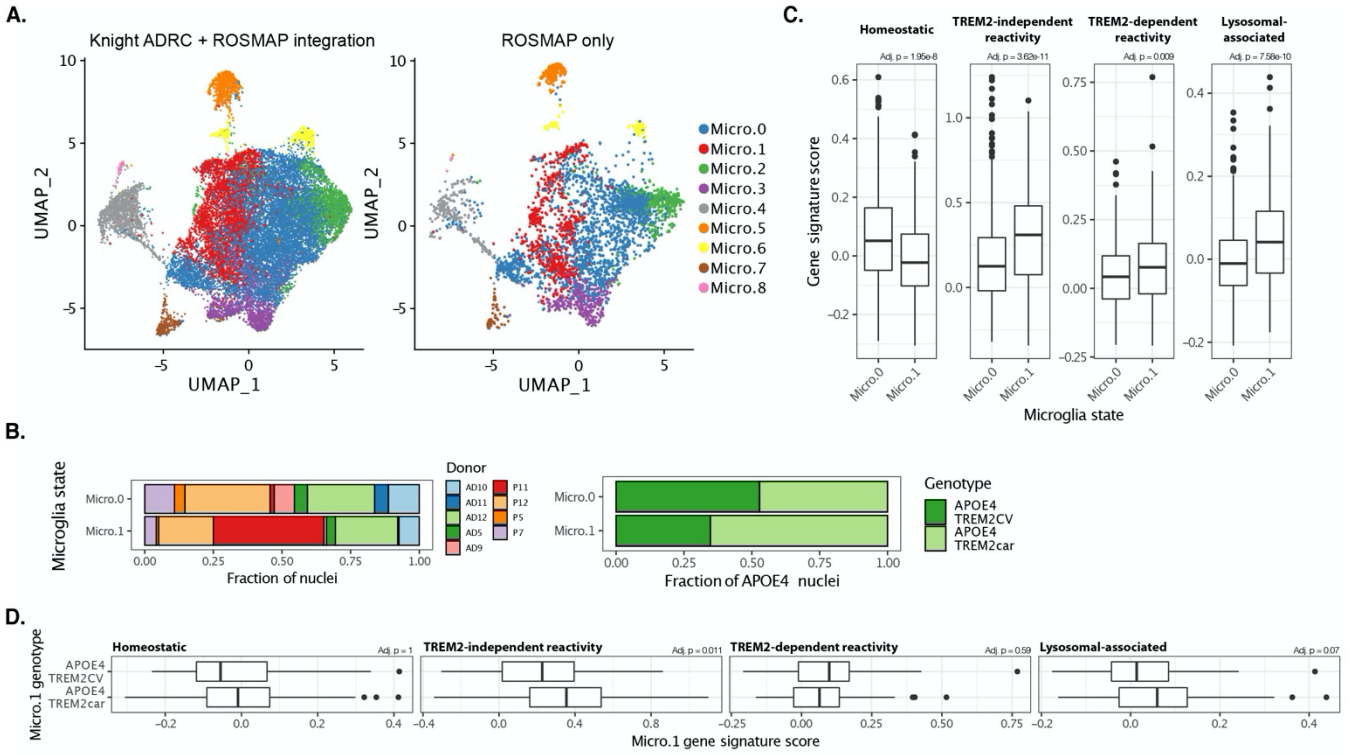

Suppl. Figure 6. Human single-nuclei RNA sequencing from AD-E4 patients display similar microglia profiles in TREM2 variant carriers (p.R47H, p.R62H) vs. TREM2 common variant carriers) (related to Figure 7). (A) UMAP representation of human microglia snRNA-seq data from ROSMAP human pre-frontal cortex tissue snRNA-seq data from the Rush Alzheimer's Disease Center [49] integrated with the Knight ADRC cohort [47]. Micro.0 corresponds to resting-state microglia, and Micro.1 corresponds to activated microglia (B) Distribution of donors and genotypes for Micro.0 and Micro.1. (C) Gene signature score comparisons between Micro.0 and Micro.1. (D) Gene signature comparisons for the signatures of interest across TREM2 genotypes. CV: TREM2 common variant; car: TREM2 carriers for R47H or R62H variants. Gene signature comparisons p-values calculated using Wilcoxon rank-sum test and adjusted for multiple testing using a Bonferroni correction.

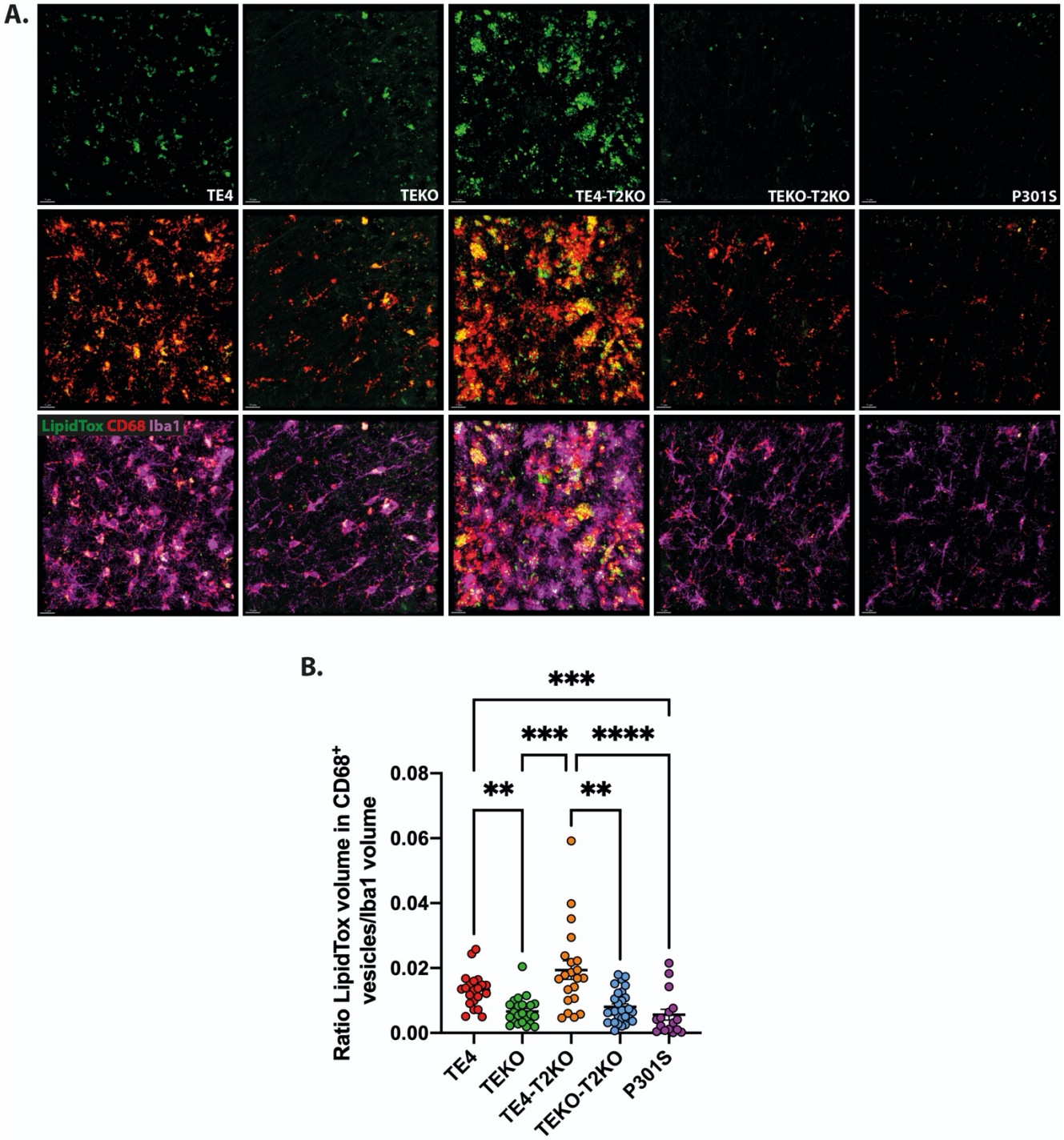

Suppl. Figure 7. Aberrant lysosomal lipid accumulation in TE4 mice with or without TREM2 deletion is human ApoE4 specific (related to Figure 6). (A) Representative images of LipidTox (green), CD68 (red) and Iba1 (purple) from HC of 9-month-old mice. Scale bars: 15 µm. (B) Quantification of the ratio of LipidTox volume within $CD68^{+}$ vesicles per Iba1 microglia volume in the hippocampus from 9-month-old mice. Data are presented as mean ± SEM. Significance was determined using a Kruskal–Wallis test followed by a Dunn's post hoc test due to the nonparametric data set for (B). **, $P < 0.01$; ***, $P < 0.001$; ****, $P < 0.0001$. (n=20-27 mice/group).

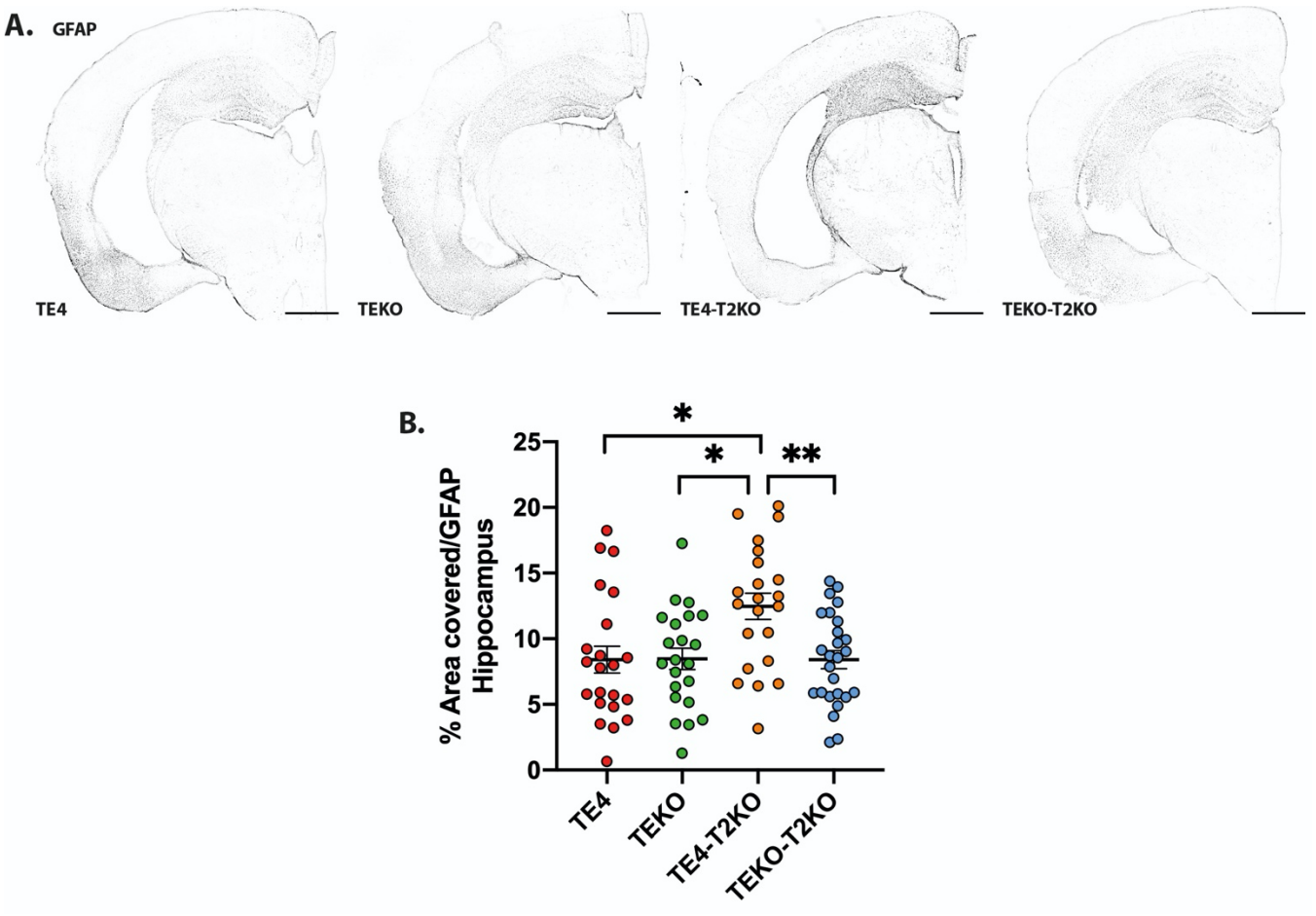

Suppl. Figure 8. TREM2 deletion increases GFAP+ astrocytes in TE4 mice, but not in TEKO mice (related to Figure 8).

(A) Representative images of GFAP (green) from 9-month-old mice. Scale bars: 1 mm (B) Quantification of the average area covered by GFAP in the hippocampus from 9-month-old mice. Data are presented as mean ± SEM. Significance was determined using a one-way ANOVA followed by a Tukey's post hoc test. *, $P < 0.0$; **, $P < 0.01$. (n=20-27 mice/group).